Photoswitchable catalysis by a self-assembled molecular cage

Ray G. DiNardi[a], Samina Rasheed[a], Simona S. Capomolla[a], M. Him Chak[a], Isis A. Middleton[a], Lauren K. Macreadie,[a] Jake P. Violi[a], William A. Donald[a], Paul J. Lusby[b]*, and Jonathon E. Beves[a]*

KEYWORDS Self-assembly · Coordination Cage · Photoswitch · Photochromism · Catalysis

ABSTRACT: A heteroleptic $[Pd_2L_2L'_2]^{4+}$ coordination cage containing a photoswitchable azobenzene-derived ligand catalyzes the Michael addition reaction between methyl vinyl ketone and benzoyl nitromethane within its cavity. The corresponding homoleptic cages are catalytically inactive. The heteroleptic cage can be reversibly disassembled and reassembled using 530 nm light and 405 nm light, respectively, allowing catalysis within the cage to be switched *OFF* and *ON* at will.

Over the past three decades, supramolecular cages have evolved from simple hosts to systems with impressive catalytic functions.[1] Inspired by how enzymes accelerate reactions, catalytic cages can leverage their activity in multiple ways. These include methods that rely on reducing the entropy of activation, for example using binding to limit conformational freedom,[2] or by encapsulating more than one substrate to increase effective concentration.[3] Cages can also use electrostatic forces to drive catalysis, for example leading to either enhanced basicity[4] or acidity[5] of the substrate compared to the non-bound species, and/or stabilizing any subsequent higher energy species.[6] Other methods of accelerating reactions include binding substrates in higher energy conformational states,[7] or using the local high concentration of ions around the cage portals.[8] When more than one of these mechanisms is used simultaneously, very high activity can be observed.[9] Molecular cages have also been used to control regioselectivity, although these reactions are not typically catalytic.[10]

A key feature of enzyme catalysis is regulated activity. This area of cage catalysis remains significantly underdeveloped and invariably relies on either the endo or exo binding of a guest that is not a substrate.[11] One way to mediate cage catalysis would be using light irradiation. Light-responsive molecular cages have been prepared using photoswitchable ligands and metal ions.[12] These include those based on diarylethene photoswitches that form cages with different geometries and cavity sizes, allowing selective guest binding.[13] Diazocine-based cages are unique as they can be switched from a thermodynamically stable *Z*-isomer to the *E*-isomer using visible light, forming metastable cages that encapsulate guests.[14] A related example uses two diazocine ligands that allow light to selectively disassemble one cage and assemble another.[15] We have recently reported an azobenzene-based molecular cage that reversibly responds to visible light to change its composition from a $[Pd_2L_4]^{4+}$ lantern-like structure to a $[PdL_2]^{2+}$ monomeric product.[16] However, guest molecules do not readily bind within the cavity of the lantern-like cage,[16] instead preferentially binding on the exterior. Molecular cages can also act as photosensitizers,[17] and have been used to drive photochemical reactions away from equilibrium.[18]

Photoswitchable catalysis[19] has progressed significantly since the earliest reports,[20] with examples of enantioselective catalysis,[21] polymerization[22] and cooperative catalysis.[23] In these examples, the catalysis is switched by changing the electronic properties of a donor atom,[24] blocking an active site with steric bulk,[20] bringing together cooperative organocatalytic groups,[21a] or forming a more reactive functional group.[25] While there are reports of switchable catalysis within macrocycles,[26] on surfaces of nanoparticles,[27] and using rotaxanes,[28] to the best of our knowledge, there are no reports of photoswitchable catalysis using discrete self-assembled species. Herein we report light-regulated catalysis using a heteroleptic $[Pd_2L_2L'_2]^{4+}$ cage system (Figure 1).

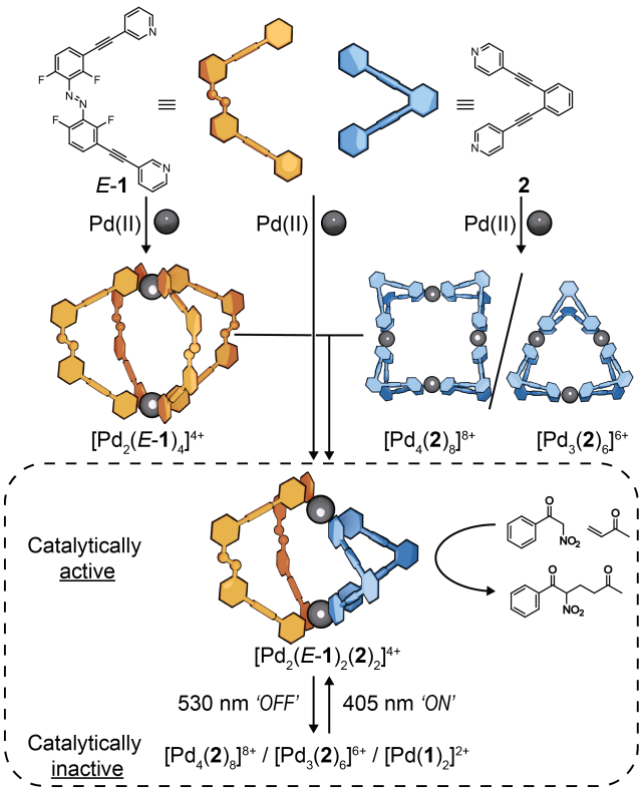

Figure 1. Self-assembly of homoleptic cages $[Pd_2(E\text{-}\mathbf{1})_4]^{4+}$, $[Pd_4(\mathbf{2})_8]^{8+}$, $[Pd_3(\mathbf{2})_6]^{6+}$ and photoswitchable heteroleptic cage catalyst $[Pd_2(E\text{-}\mathbf{1})_2(\mathbf{2})_2]^{4+}$.

Photoswitchable ligand **1** was synthesized via Sonogashira cross-coupling (see SI S2) of 3–bromo–2,6–difluoroaniline

and 3-ethynylpyridine to give 2,6-difluoro-3-(pyridin-3-ylethynyl)aniline in 80% yield. The reaction of two equivalents of this aniline with *N*-chlorosuccinimide (NCS) and 1,8-diazabicyclo[5.4.0]undec-7-ene (DBU)[29] gave photoswitchable ligand **1** in 33% yield. A single-crystal X-ray structure of *E*-**1** (CCDC: 2343887, see SI S2.4) confirmed the rings are almost coplanar, like related ligands we have reported.[16, 30]

The photoswitching properties of ligand **1** were investigated using NMR and UV-vis absorption spectroscopies (see SI S3). Photostationary states (PSS) were generated by irradiating a sample of *E*-**1** in DMSO-d_6 with a 530 nm LED for 10 minutes (PSS_{530} = 88% *Z*-**1**) or 405 nm LED for 20 minutes (PSS_{405} = 86% *E*-**1**). The metastable isomer, *Z*-**1**, has a thermal half-life of around a month at room temperature in DMSO (see SI S3.3), in line with that of related switches.[16]

Reaction of ligand *E*-**1** (4.6 mM, 1 equiv.) and $[Pd(MeCN)_4](BF_4)_2$ (2.3 mM, 0.5 equiv.) in DMSO-d_6 gives the homoleptic lantern-like complex $[Pd_2(E\text{-}\mathbf{1})_4](BF_4)_4$, as shown by the combination of NMR spectroscopy (Figure 2a) and electrospray ionization mass spectrometry (ESI-MS) (see SI S6). When $[Pd_2(E\text{-}\mathbf{1})_4](BF_4)_4$ in DMSO-d_6 is irradiated with 530 nm light, the monomeric complex $[Pd(Z\text{-}\mathbf{1})_2](BF_4)_2$ is formed, as confirmed by NMR and ESI-MS experiments (see SI S7). This behavior is analogous to that of a related $[Pd_2L_4](BF_4)_4$ cage.[16] With this favorable photochemical switching, the host-guest chemistry of $[Pd_2(E\text{-}\mathbf{1})_4]^{4+}$ was then explored using the analogous tetrakis[3,5-bis(trifluoromethyl)phenyl]borate (BAr_F) salt.[31] The use of these large, "greasy" counteranions facilitates both host-guest chemistry[31] and catalysis[1e] with simple Pd_2L_4 cages. This is because they maximize polar (and electrostatically activating) interactions in less polar solvents by removing competitive counteranion binding.

To prepare the BAr_F salt, *E*-**1** was reacted with $[Pd(Py^*)_4](BAr_F)_2$ (where Py* = 3-chloropyridine, see SI S4)[32] in acetonitrile to give $[Pd_2(E\text{-}\mathbf{1})_4](BAr_F)_4$, which was characterized by NMR and ESI-MS data (see SI S6.4, S6.5). Disappointingly, $[Pd_2(E\text{-}\mathbf{1})_4](BAr_F)_4$ showed little evidence of guest binding, nor was it able to catalyze the representative Michael addition reaction of methyl vinyl ketone and benzoyl nitromethane in the presence of 18-crown-6, similar to the behavior of a related cage[16] (SI S5.2, S5.3, S18.4.3).

There are several possible reasons for this lack of host-guest chemistry and reactivity. It could be that the relative size and shape of the cavity of $[Pd_2(E\text{-}\mathbf{1})_4](BAr_F)_4$ is unsuitable for encapsulating the substrates. A molecular model of the homoleptic cage also reveals another potential problem; $[Pd_2(E\text{-}\mathbf{1})_4]^{4+}$ likely has a pronounced twisted conformation (Figure 2b), a consequence of the non-parallel coordination vectors of *E*-**1**, similar to a related cage.[16] It has previously been shown that guest binding inside non-twisted, D_{4h} symmetric Pd_2L_4 cages is facilitated by the formation of hydrogen bonds with the two sets of four polarized *ortho*-pyridyl protons that point directly into the cavity.[31] These interactions also drive Michael addition catalysis by stabilizing the deprotonated nucleophile and co-binding the electrophile to reduce the entropy of activation.[33] In the case of $[Pd_2(E\text{-}1)_4]^{4+}$, we attribute the lack of host-guest chemistry and catalysis to the twisted, propeller-like conformation of the $Pd(pyridyl)_4$ units.

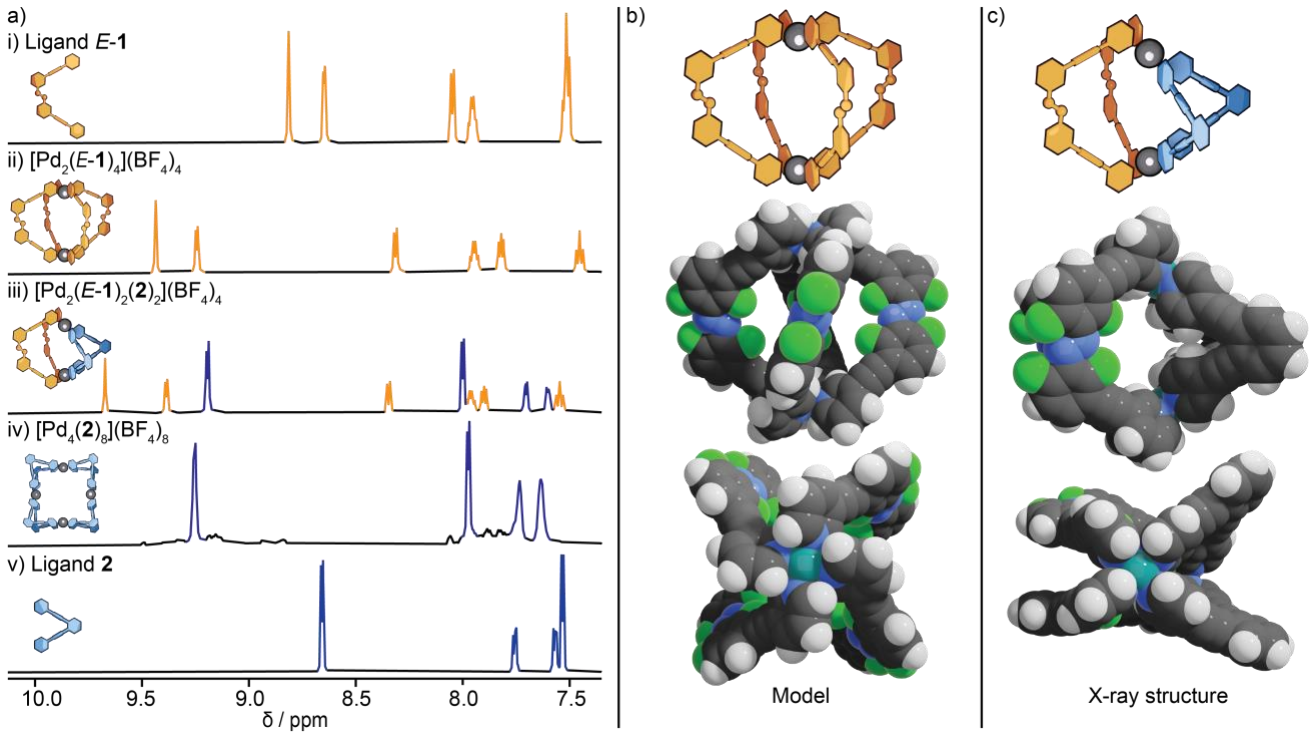

Figure 2. Characterization of homoleptic and heteroleptic cages. a) ^{1}H NMR spectra (600 MHz, DMSO-d_6) of i) photoswitchable ligand *E*-**1**; ii) homoleptic $[Pd_2(E\text{-}\mathbf{1})_4](BF_4)_4$; iii) heteroleptic $[Pd_2(E\text{-}\mathbf{1})_2(\mathbf{2})_2](BF_4)_4$; iv) homoleptic $[Pd_4(\mathbf{2})_8](BF_4)_8$ and $[Pd_3(\mathbf{2})_6](BF_4)_6$, as reported[34]; v) ligand **2**. b) Molecular mechanics model of homoleptic $[Pd_2(E\text{-}\mathbf{1})_4](BF_4)_4$. c) Single crystal X-ray structure of heteroleptic $[Pd_2(E\text{-}\mathbf{1})_2(\mathbf{2})_2](BF_4)_4$, CCDC: 2343886. Color codes: grey: carbon; white: hydrogen; blue: nitrogen; green: fluorine; teal: palladium. Anions and solvent molecules are omitted for clarity.

This twisting perturbs the convergent cavity-directed hydrogen-bond donor atoms, hindering the formation of favorable electrostatic interaction that infer catalytic activity.

Looking at an alternative cage design, and to address the twisted conformation that could hinder catalysis, we targeted a heteroleptic system combining rigid ligand **2** with *E*-**1**. This combination of ligands was selected for their shape complementarity.[35] On its own, ligand **2** is reported[34] to react with palladium(II) ions to form a $[Pd_3(\mathbf{2})_6]^{6+}$ double-walled triangle in acetonitrile and a $[Pd_4(\mathbf{2})_8]^{8+}$ double-walled square in DMSO and never a $[Pd_2(\mathbf{2})_4]^{4+}$ dimer, which is also our observations (Figure 2aiv, SI S8 and S9).[34]

When one equivalent of each of ligand *E*-**1**, ligand **2**, and $[Pd(MeCN)_4](BF_4)_2$ are combined in DMSO-d_6 a single new species is formed within 10 min at room temperature (Figure 2aiii, SI S10). An identical result is obtained if the homoleptic cages $[Pd_2(E\text{-}\mathbf{1})_4](BF_4)_4$ and $[Pd_4(\mathbf{2})_8](BF_4)_8$ are combined in DMSO-d_6 and heated with a heat gun for 5 min (see SI S10.1), indicating that the heteroleptic cage is the thermodynamic product. Multinuclear NMR experiments (SI S10.2) confirm the heteroleptic cage is symmetrical with a single environment for each of the ligands, *E*-**1** and **2**. Inter-ligand ROESY interactions indicate that both ligands are coordinated to the same metal ion (SI S10.2).

Diffusion NMR experiments in DMSO-d_6 (see SI S13) gave hydrodynamic radii in line with expectations: $[Pd_2(E\text{-}\mathbf{1})_2(\mathbf{2})_2]^{4+}$ (9.1 nm), smaller than that of the homoleptic $[Pd_2(E\text{-}\mathbf{1})_4]^{4+}$ (10.5 nm) and the macrocyclic $[Pd_4(\mathbf{2})_8]^{8+}$ (9.9 nm). ESI-MS confirmed the composition as $[Pd_2(\mathbf{1})_2(\mathbf{2})_2]^{4+}$ with a series of ions with isotope patterns corresponding to sequential loss of BF_4 anions (SI S10.3).

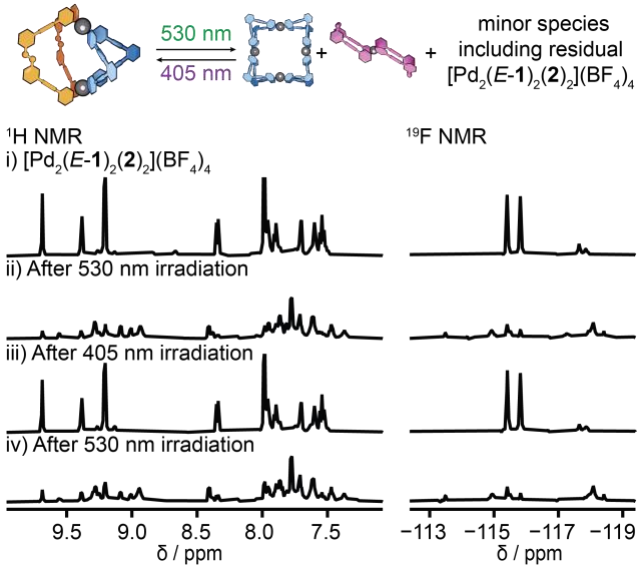

Figure 3. Partial ^{1}H (600 MHz) and ^{19}F (565 MHz) NMR spectra in DMSO-d_6 showing photoswitching of heteroleptic cage $[Pd_2(E\text{-}\mathbf{1})_2(\mathbf{2})_2](BF_4)_4$ i) before irradiation; ii) after 530 nm 10 min; iii) 405 nm 5 min; iv) 530 nm 10 min irradiation. The PSS composition (PSS_{530} = 88% *Z*-**1**, the same as for the free ligand **1**) was confirmed by adding *N*,*N*-dimethyl-4-aminopyridine (DMAP) to displace the ligands. See SI S11.3 for details.

Finally, a single crystal suitable for X-ray diffraction unambiguously confirmed the heteroleptic species as *cis*-$[Pd_2(E\text{-}\mathbf{1})_2(\mathbf{2})_2](BF_4)_4$ (Figure 2c, CCDC: 2343886, SI S10.4), in line with expectations from shape complementarity prediction.[35] The cage has a Pd···Pd separation of 9.92 Å, and has a BF_4^- anion inside the cavity, confirming its ability to bind guests. The pyridyl units are not significantly twisted (angles between the *trans* pyridyl rings range from 16 to 22 °), and therefore the *ortho*-pyridyl hydrogen-bond donors project into the cavity for optimal guest binding and catalysis.

When the heteroleptic cage $[Pd_2(E\text{-}\mathbf{1})_2(\mathbf{2})_2](BF_4)_4$ in DMSO-d_6 is irradiated with 530 nm light it is disassembled, and the ^{1}H NMR spectrum (Figure 3ii) shows a mixture of products is formed. The mixture includes $[Pd(Z\text{-}\mathbf{1})_2]^{2+}$ and $[Pd_4(\mathbf{2})_8]^{8+}$, and possibly $[Pd_2(Z\text{-}\mathbf{1})_2(\mathbf{2})_2]^{4+}$ (SI S11). Upon irradiating with 405 nm light the heteroleptic cage $[Pd_2(E\text{-}\mathbf{1})_2(\mathbf{2})_2](BF_4)_4$ is reformed near quantitatively (Figure 3iii, SI S11.3). This data confirms heteroleptic cage $[Pd_2(E\text{-}\mathbf{1})_2(\mathbf{2})_2](BF_4)_4$ can be reversibly assembled and disassembled using visible light.

Turning to the equivalent BAr_F salt, we then tested whether the heteroleptic cage $[Pd_2(E\text{-}\mathbf{1})_2(\mathbf{2})_2](BAr_F)_4$ could be formed, and in particular, whether it could be generated from the re-arrangement of the two homoleptic structures. Homoleptic structures $[Pd_2(E\text{-}\mathbf{1})_4](BAr_F)_4$ and $[Pd_3(\mathbf{2})_6](BAr_F)_6$/$[Pd_4(\mathbf{2})_8](BAr_F)_8$ can be assembled with $[Pd(Py^*)_4](BAr_F)_2$ in CD_3CN, and were characterized by NMR (SI S6.4, S9.4) and ESI-MS data (SI S6.5, S9.5). When a 1:1 mixture of these two homoleptic cages was combined in CD_3CN and heated at 50 °C for 30 min, the heteroleptic cage was formed quantitatively (SI S10.5). This indicates that swapping from BF_4 to BAr_F counteranions does not lead to problems of kinetic trapping. However, the solvent that is optimal for this catalysis—dichloromethane—is poorly coordinating and therefore does not promote the rapid ligand exchange required for cage switching. We found that a solvent mixture of 11:1 CD_2Cl_2/CD_3CN, was a good compromise to maximize the host-guest chemistry while providing some coordinating properties to facilitate cage rearrangement (see SI S14, S15).

Using these mixed solvent conditions, we investigated the binding of methyl vinyl ketone and benzoyl nitromethane within $[Pd_2(E\text{-}\mathbf{1})_2(\mathbf{2})_2](BAr_F)_4$ (SI S17) as well as the ability of $[Pd_2(E\text{-}\mathbf{1})_2(\mathbf{2})_2](BAr_F)_4$ to catalyze the Michael addition reaction between these two substrates (SI S18).[36] When methyl vinyl ketone is added to a sample of the heteroleptic cage only minor shifts were observed in the ^{1}H NMR peaks of the cage, with no substantial changes when 18-crown-6 is also added (see SI 17.1). By contrast when benzoyl nitromethane is added a new set of deshielded signals are observed that correspond to the cage with bound deprotonated benzoyl nitromethane. These signals increase in intensity once 18-crown-6 is added (see SI 17.2). The signals that show the biggest difference in chemical shift compared to the "empty cage" correspond to the protons adjacent to the pyridyl nitrogen of the non-switchable ligand **2**, and of the inwardly directed *ortho*-pyridyl CH of the photoswitchable ligand **1**. These chemical shift differences are in line with those observed from simple Pd_2L_4 cages[1e, 5, 31] and are consistent with the binding of the substrates inside the cage through CH···O hydrogen bonds (Figure 4a). We have also found that triflate binds tightly inside the cage, similarly evidenced by the appearance of a second set of cage signals with deshielded inward-facing proton resonances (SI S17.4).

When both substrates are present this clear indication of substrate binding is accompanied by substrate consumption and the generation of the Michael addition product, as monitored using ^{1}H NMR spectroscopy (Figure 4, SI S18). An 11% catalyst loading heteroleptic species $[Pd_2(\textit{E}\text{-}\mathbf{1})_2(\mathbf{2})_2](BAr_F)_4$ converted 24% of the benzoyl nitromethane to the Michael addition product in 10 hours.

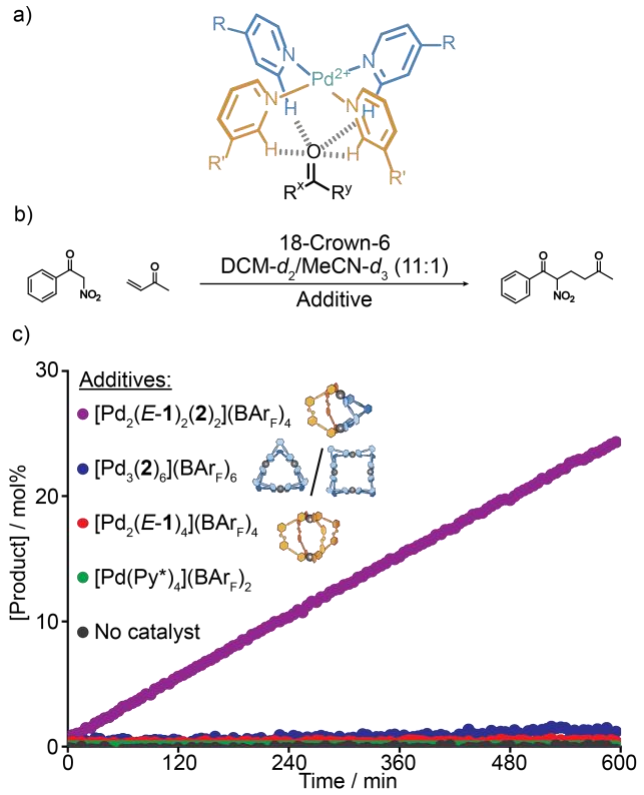

Figure 4. Catalysis of a Michael addition reaction by self-assembled cages. a) Substrate binding inside the heteroleptic cage via CH···O hydrogen bonds. b) Michael addition reaction between benzoyl nitromethane and methyl vinyl ketone. c) Michael addition reaction with different additives. Reaction conditions: CD_2Cl_2/CD_3CN (11:1), benzoyl nitromethane (14 mM), methyl vinyl ketone (27 mM), and 18-crown-6 (11 mM). All cases with palladium [Pd] = 1.6 mM. Product formation measured by ^{1}H NMR spectroscopy. See SI S18.4.

Having already found that the homoleptic photoswitchable cage $[Pd_2(\textit{E}\text{-}\mathbf{1})_4](BAr_F)_4$ is not a catalyst (see above), we also tested whether $[Pd_3(\mathbf{2})_6](BAr_F)_6$/$[Pd_4(\mathbf{2})_8](BAr_F)_8$ would show any reactivity. These homoleptic species also showed virtually no catalysis, with <1% benzoyl nitromethane going to the product over 10 hours. To ensure $[Pd_2(\textit{E}\text{-}\mathbf{1})_2(\mathbf{2})_2](BAr_F)_4$ was responsible for the catalysis, control experiments were performed using no catalyst and with $[Pd(Py^*)_4](BAr_F)_2$. For both control experiments, no product formation was observed. Crucially, we have also found that the addition of one equivalent of the strongly binding triflate guest to the $[Pd_2(\textit{E}\text{-}\mathbf{1})_2(\mathbf{2})_2](BAr_F)_4$ catalyzed transformation effectively halts reactivity (SI S19.5). This observation provides further strong support for a mechanism that involves substrate encapsulation.

Having shown that we can reversibly switch the heteroleptic cage with light and that it is also an active catalyst, it was time for photoswitchable catalysis! The $[Pd_2(\textit{E}\text{-}\mathbf{1})_2(\mathbf{2})_2](BAr_F)_4$ cage was successfully disassembled (530 nm light for 10 min) and reassembled (405 nm light for 5 min) in 11:1 CD_2Cl_2/CD_3CN (see SI S19), showing similar behavior to the BF_4 salt in DMSO-d_6 (Figure 3).[31] Benzoyl nitromethane, methyl vinyl ketone and 18-crown-6 were added to the sample and the reaction was monitored using ^{1}H NMR spectroscopy (Figure 5a), showing the cage was catalytically active. Next, the sample was irradiated with a 530 nm LED for 10 min, which resulted in a 10-fold decrease in the rate of product formation as the cage was disassembled. The reaction was then reactivated by irradiating with a 405 nm LED for 5 min. Following this reactivation, the rate of product formation was almost identical to that prior to 530 nm irradiation, showing that the photoswitching is completely reversible.

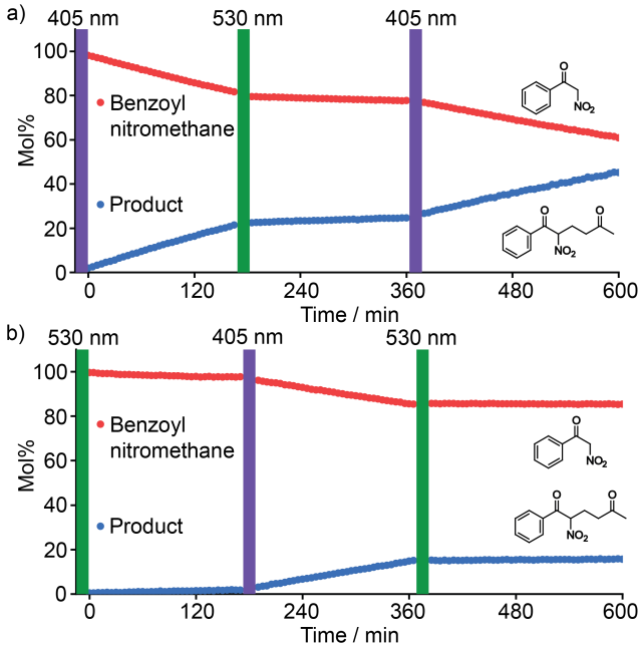

Figure 5. Photoswitchable catalysis by the heteroleptic cage $[Pd_2(\textit{E}\text{-}\mathbf{1})_2(\mathbf{2})_2](BAr_F)_4$ in CD_2Cl_2:CD_3CN 11:1 monitored by ^{1}H NMR spectroscopy. a) ON/OFF/ON cycle and b) OFF/ON/OFF cycle. Reaction conditions: benzoyl nitromethane (17 mM), methyl vinyl ketone (33 mM), and 18-crown-6 (12 mM), [Pd] 2.0 mM. Irradiation by 405 nm (5 min) and 530 (10 min) outside of the NMR instrument, with colored bars representing the time between NMR measurements, see SI S19 for details.

The system can also be kept dormant by first irradiating $[Pd_2(\textit{E}\text{-}\mathbf{1})_2(\mathbf{2})_2](BAr_F)_4$ with a 530 nm LED before the substrates are added (Figure 5b, SI S19.3). The reaction can then be activated at will by irradiating the sample with a 405 nm LED. The long thermal half-life of the photoswitch ensures the cage remains in the state it is programmed after the irradiation is stopped. The responsiveness of the system to visible light demonstrates that using a molecular photoswitch to control self-assembly can lead to excellent control of chemical reactivity. We also show that the system can be subjected to at least five cycles of photoswitching without any effect on catalytic performance (SI S19.4).

In conclusion, we have shown the first example of photoswitchable catalysis within a self-assembled molecular cage. The mechanism of catalysis relies on electrostatic interactions within the cavity, which is only possible in the heteroleptic cage with a cavity preorganized for guest binding.

The catalysis can be switched on and off with visible light (405 nm and 530 nm respectively) and is entirely reversible. Controlling the catalytic activity of self-assembled cavities with non-destructive visible light is a new method for directing chemical reactions. Combining photoswitchable ligands with facile ligand-exchange reactions allows a system to be driven towards assemblies comprised of different components, with programmable stoichiometries, shapes, affinities and now catalytic functions. We anticipate future examples could include different self-assembled cages each capable of catalyzing different reactions, allowing more complex multi-step reactions to be performed simply by using visible light.

ASSOCIATED CONTENT

SUPPORTING INFORMATION

Experimental data, spectra and other data are supplied as Supporting Information

AUTHOR INFORMATION

Corresponding Authors

Jonathon E. Beves j.beves@unsw.edu.au
Paul J. Lusby* Paul.Lusby@ed.ac.uk
[a]*School of Chemistry, UNSW Sydney, Sydney, New South Wales 2052, Australia*
[b]*EaStCHEM School of Chemistry, University of Edinburgh, Joseph Black Building, David Brewster Road, Edinburgh, Scotland, EH9 3FJ, U.K*

Author Contributions

The manuscript was written through contributions of all authors.

ACKNOWLEDGMENT

The Australian Research Council is acknowledged for funding (DP220101847, DE210101627), The Mark Wainright Analytical Centre's NMR facility, and the Australian Synchrotron, part of ANSTO, for access to the MX2 beamline (CAP19108), and made use of the Australian Cancer Research Foundation (ACRF) detector. P.J.L acknowledge EPSRC for funding (EP/W010666/1).

REFERENCES

(1) a) Kang, J.; Rebek, J. Acceleration of a Diels–Alder reaction by a self-assembled molecular capsule. *Nature* **1997**, *385* (6611), 50-52. DOI: 10.1038/385050a0. b) Kang, J.; Santamaría, J.; Hilmersson, G.; Rebek, J. Self-Assembled Molecular Capsule Catalyzes a Diels−Alder Reaction. *J. Am. Chem. Soc.* **1998**, *120* (29), 7389-7390. DOI: 10.1021/ja980927n. c) Hooley, R. J.; Rebek, J. A deep cavitand catalyzes the Diels-Alder reaction of bound maleimides. *Org. Biomol. Chem.* **2007**, *5* (22), 3631-3636. DOI: 10.1039/b713104f. d) Zhang, Q.; Tiefenbacher, K. Terpene cyclization catalysed inside a self-assembled cavity. *Nat. Chem.* **2015**, *7* (3), 197-202. DOI: 10.1038/nchem.2181. e) Marti-Centelles, V.; Lawrence, A. L.; Lusby, P. J. High Activity and Efficient Turnover by a Simple, Self-Assembled "Artificial Diels-Alderase". *J. Am. Chem. Soc.* **2018**, *140* (8), 2862-2868. DOI: 10.1021/jacs.7b12146. f) Grommet, A. B.; Feller, M.; Klajn, R. Chemical reactivity under nanoconfinement. *Nat. Nanotechnol.* **2020**, *15* (4), 256-271. DOI: 10.1038/s41565-020-0652-2. g) Piskorz, T. K.; Martí-Centelles, V.; Spicer, R. L.; Duarte, F.; Lusby, P. J. Picking the lock of coordination cage catalysis. *Chem. Sci.* **2023**, *14* (41), 11300-11331. DOI: 10.1039/D3SC02586A. h) Dorrat, J. C.; Taylor, C. G. P.; Young, R. J.; Solea, A. B.; Turner, D. R.; Dennison, G. H.; Ward, M. D.; Tuck, K. L. A Study on Auto-Catalysis and Product Inhibition: A Nucleophilic Aromatic Substitution Reaction Catalysed within the Cavity of an Octanuclear Coordination Cage. *Chem.- Eur. J.* **2024**. DOI: 10.1002/chem.202400501.

(2) a) Fiedler, D.; Bergman, R. G.; Raymond, K. N. Supramolecular Catalysis of a Unimolecular Transformation: Aza-Cope Rearrangement within a Self-Assembled Host. *Angew. Chem. Int. Ed.* **2004**, *43* (48), 6748-6751. DOI: 10.1002/anie.200461776. b) Genov, G. R.; Takezawa, H.; Hayakawa, H.; Fujita, M. Tetradehydro-Diels–Alder Reactions of Flexible Arylalkynes via Folding Inside a Molecular Cage. *J. Am. Chem. Soc.* **2023**, *145* (31), 17013-17017. DOI: 10.1021/jacs.3c06301.

(3) a) Yoshizawa, M.; Tamura, M.; Fujita, M. Diels-Alder in Aqueous Molecular Hosts: Unusual Regioselectivity and Efficient Catalysis. *Science* **2006**, *312* (5771), 251-254. DOI: doi:10.1126/science.1124985. b) Murase, T.; Horiuchi, S.; Fujita, M. Naphthalene Diels−Alder in a Self-Assembled Molecular Flask. *J. Am. Chem. Soc.* **2010**, *132* (9), 2866-2867. DOI: 10.1021/ja9107275. c) Horiuchi, S.; Murase, T.; Fujita, M. Diels-Alder Reactions of Inert Aromatic Compounds within a Self-Assembled Coordination Cage. *Chem.- Asian J.* **2011**, *6* (7), 1839-1847. DOI: 10.1002/asia.201000842.

(4) Pluth, M. D.; Bergman, R. G.; Raymond, K. N. Acid Catalysis in Basic Solution: A Supramolecular Host Promotes Orthoformate Hydrolysis. *Science* **2007**, *316* (5821), 85-88. DOI: 10.1126/science.1138748.

(5) Wang, J.; Young, T. A.; Duarte, F.; Lusby, P. J. Synergistic Noncovalent Catalysis Facilitates Base-Free Michael Addition. *J. Am. Chem. Soc.* **2020**, *142* (41), 17743-17750. DOI: 10.1021/jacs.0c08639.

(6) a) Murase, T.; Nishijima, Y.; Fujita, M. Cage-Catalyzed Knoevenagel Condensation under Neutral Conditions in Water. *J. Am. Chem. Soc.* **2012**, *134* (1), 162-164. DOI: 10.1021/ja210068f. b) Bolliger, J. L.; Belenguer, A. M.; Nitschke, J. R. Enantiopure Water-Soluble [Fe4L6] Cages: Host–Guest Chemistry and Catalytic Activity. *Angew. Chem. Int. Ed.* **2013**, *52* (31), 7958-7962. DOI: 10.1002/anie.201302136. c) Spicer, R. L.; Stergiou, A. D.; Young, T. A.; Duarte, F.; Symes, M. D.; Lusby, P. J. Host-Guest-Induced Electron Transfer Triggers Radical-Cation Catalysis. *J. Am. Chem. Soc.* **2020**, *142* (5), 2134-2139. DOI: 10.1021/jacs.9b11273.

(7) Takezawa, H.; Shitozawa, K.; Fujita, M. Enhanced reactivity of twisted amides inside a molecular cage. *Nat. Chem.* **2020**, *12* (6), 574-578. DOI: 10.1038/s41557-020-0455-y.

(8) a) Cullen, W.; Misuraca, M. C.; Hunter, C. A.; Williams, N. H.; Ward, M. D. Highly efficient catalysis of the Kemp elimination in the cavity of a cubic coordination cage. *Nat. Chem.* **2016**, *8* (3), 231-236. DOI: 10.1038/nchem.2452. b) Cullen, W.; Metherell, A. J.; Wragg, A. B.; Taylor, C. G. P.; Williams, N. H.; Ward, M. D. Catalysis in a Cationic Coordination Cage Using a Cavity-Bound Guest and Surface-Bound Anions: Inhibition, Activation, and Autocatalysis. *J. Am. Chem. Soc.* **2018**, *140* (8), 2821-2828. DOI: 10.1021/jacs.7b11334.

(9) Hastings, C. J.; Pluth, M. D.; Bergman, R. G.; Raymond, K. N. Enzymelike Catalysis of the Nazarov Cyclization by Supramolecular Encapsulation. *J. Am. Chem. Soc.* **2010**, *132* (20), 6938-6940. DOI: 10.1021/ja102633e.

(10) a) Iizuka, K.; Takezawa, H.; Fujita, M. Chemical Site-Differentiation of Calix[4]arenes through Enforced Conformations by Confinement in a Cage. *J. Am. Chem. Soc.* **2023**, *145* (48), 25971-25975. DOI: 10.1021/jacs.3c10720. b) Lu, Z.; Ronson, T. K.; Heard, A. W.; Feldmann, S.; Vanthuyne, N.; Martinez, A.; Nitschke, J. R. Enantioselective fullerene functionalization through stereochemical information transfer from a self-assembled cage. *Nat. Chem.* **2023**, *15* (3), 405-412. DOI: 10.1038/s41557-022-01103-y.

(11) Martí-Centelles, V.; Spicer, R. L.; Lusby, P. J. Non-covalent allosteric regulation of capsule catalysis. *Chem. Sci.* **2020**, *11* (12), 3236-3240. DOI: 10.1039/D0SC00341G.

(12) a) Nieland, E.; Voss, J.; Schmidt, B. M. Photoresponsive Supramolecular Cages and Macrocycles. *ChemPlusChem* **2023**, *88* (12), e202300353. DOI: 10.1002/cplu.202300353. b) Wezenberg, S. J. Light-switchable Metal-Organic Cages. *Chem. Lett.* **2020**, *49* (6),

609-615. DOI: 10.1246/cl.200076 (acccessed 6/10/2024). c) Lin, H.-Y.; Wang, Y.-T.; Shi, X.; Yang, H.-B.; Xu, L. Switchable metallacycles and metallacages. *Chem. Soc. Rev.* **2023**, *52* (3), 1129-1154, 10.1039/D2CS00779G. DOI: 10.1039/D2CS00779G. d) Benchimol, E.; Tessarolo, J.; Clever, G. H. Photoswitchable coordination cages. *Nat. Chem.* **2024**, *16* (1), 13-21. DOI: 10.1038/s41557-023-01387-8.

(13) a) Han, M. X.; Michel, R.; He, B.; Chen, Y. S.; Stalke, D.; John, M.; Clever, G. H. Light-Triggered Guest Uptake and Release by a Photochromic Coordination Cage. *Angew. Chem. Int. Ed.* **2013**, *52* (4), 1319-1323. DOI: 10.1002/anie.201207373. b) Li, R. J.; Han, M. X.; Tessarolo, J.; Holstein, J. J.; Lübben, J.; Dittrich, B.; Volkmann, C.; Finze, M.; Jenne, C.; Clever, G. H. Successive Photoswitching and Derivatization Effects in Photochromic Dithienylethene-Based Coordination Cages. *ChemPhotoChem* **2019**, *3* (6), 378-383. DOI: 10.1002/cptc.201900038. c) Li, R. J.; Holstein, J. J.; Hiller, W. G.; Andréasson, J.; Clever, G. H. Mechanistic Interplay between Light Switching and Guest Binding in Photochromic Pd_2Dithienylethene$_4$ Coordination Cages. *J. Am. Chem. Soc.* **2019**, *141* (5), 2097-2103. DOI: 10.1021/jacs.8b11872. d) Li, R.-J.; Tessarolo, J.; Lee, H.; Clever, G. H. Multi-stimuli Control over Assembly and Guest Binding in Metallo-supramolecular Hosts Based on Dithienylethene Photoswitches. *J. Am. Chem. Soc.* **2021**, *143* (10), 3865-3873. DOI: 10.1021/jacs.0c12188. e) Artmann, K.; Li, R. J.; Juber, S.; Benchimol, E.; Schafer, L. V.; Clever, G. H.; Nuernberger, P. Steering the Ultrafast Opening and Closure Dynamics of a Photochromic Coordination Cage by Guest Molecules. *Angew. Chem. Int. Ed.* **2022**, *61* (49), e202212112. DOI: 10.1002/anie.202212112.

(14) Lee, H.; Tessarolo, J.; Langbehn, D.; Baksi, A.; Herges, R.; Clever, G. H. Light-Powered Dissipative Assembly of Diazocine Coordination Cages. *J. Am. Chem. Soc.* **2022**, *144* (7), 3099-3105. DOI: 10.1021/jacs.1c12011.

(15) Hugenbusch, D.; Lehr, M.; von Glasenapp, J.-S.; McConnell, A. J.; Herges, R. Light-Controlled Destruction and Assembly: Switching between Two Differently Composed Cage-Type Complexes. *Angew. Chem. Int. Ed.* **2023**, *62* (1), e202212571. DOI: 10.1002/anie.202212571.

(16) DiNardi, R. G.; Douglas, A. O.; Tian, R.; Price, J. R.; Tajik, M.; Donald, W. A.; Beves, J. E. Visible-Light-Responsive Self-Assembled Complexes: Improved Photoswitching Properties by Metal Ion Coordination. *Angew. Chem. Int. Ed.* **2022**, *61* (38), e202205701. DOI: 10.1002/anie.202205701.

(17) Dalton, D. M.; Ellis, S. R.; Nichols, E. M.; Mathies, R. A.; Toste, F. D.; Bergman, R. G.; Raymond, K. N. Supramolecular Ga4L612– Cage Photosensitizes 1,3-Rearrangement of Encapsulated Guest via Photoinduced Electron Transfer. *J. Am. Chem. Soc.* **2015**, *137* (32), 10128-10131. DOI: 10.1021/jacs.5b06317.

(18) Gemen, J.; Church, J. R.; Ruoko, T. P.; Durandin, N.; Bialek, M. J.; Weissenfels, M.; Feller, M.; Kazes, M.; Odaybat, M.; Borin, V. A.; et al. Disequilibrating azobenzenes by visible-light sensitization under confinement. *Science* **2023**, *381* (6664), 1357-1363. DOI: 10.1126/science.adh9059.

(19) a) Stoll, R. S.; Hecht, S. Artificial Light-Gated Catalyst Systems. *Angew. Chem. Int. Ed.* **2010**, *49* (30), 5054-5075. DOI: 10.1002/anie.201000146. b) Göstl, R.; Senf, A.; Hecht, S. Remote-controlling chemical reactions by light: Towards chemistry with high spatio-temporal resolution. *Chem. Soc. Rev.* **2014**, *43* (6), 1982-1996. DOI: 10.1039/C3CS60383K. c) Lifschitz, A. M.; Young, R. M.; Mendez-Arroyo, J.; Stern, C. L.; McGuirk, C. M.; Wasielewski, M. R.; Mirkin, C. A. An allosteric photoredox catalyst inspired by photosynthetic machinery. *Nat. Commun.* **2015**, *6* (1), 6541. DOI: 10.1038/ncomms7541. d) Kathan, M.; Hecht, S. Photoswitchable molecules as key ingredients to drive systems away from the global thermodynamic minimum. *Chem. Soc. Rev.* **2017**, *46* (18), 5536-5550. DOI: 10.1039/C7CS00112F. e) Dorel, R.; Feringa, B. Photoswitchable catalysis based on the isomerisation of double bonds. *Chem. Commun.* **2019**, *55* (46), 6477-6486. DOI: 10.1039/c9cc01891c. f) Thaggard, G. C.; Haimerl, J.; Fischer, R. A.; Park, K. C.; Shustova, N. B. Traffic Lights for Catalysis: Stimuli-Responsive Molecular and Extended Catalytic Systems. *Angew. Chem. Int. Ed.* **2023**, *62* (29), e202302859. DOI: 10.1002/anie.202302859.

(20) Ueno, A.; Takahashi, K.; Osa, T. Photoregulation of catalytic activity of β-cyclodextrin by an azo inhibitor. *J. Chem. Soc., Chem. Commun.* **1980**, (17), 837-838. DOI: 10.1039/C39800000837.

(21) a) Wang, J. B.; Feringa, B. L. Dynamic Control of Chiral Space in a Catalytic Asymmetric Reaction Using a Molecular Motor. *Science* **2011**, *331* (6023), 1429-1432. DOI: 10.1126/science.1199844. b) Pizzolato, S. F.; Stacko, P.; Kistemaker, J. C. M.; van Leeuwen, T.; Feringa, B. L. Phosphoramidite-based photoresponsive ligands displaying multifold transfer of chirality in dynamic enantioselective metal catalysis. *Nat. Catal.* **2020**, *3* (6), 488-496. DOI: 10.1038/s41929-020-0452-y.

(22) Eisenreich, F.; Kathan, M.; Dallmann, A.; Ihrig, S. P.; Schwaar, T.; Schmidt, B. M.; Hecht, S. A photoswitchable catalyst system for remote-controlled (co)polymerization in situ. *Nat. Catal.* **2018**, *1* (7), 516-522. DOI: 10.1038/s41929-018-0091-8.

(23) Cacciapaglia, R.; Di Stefano, S.; Mandolini, L. The bis-barium complex of a butterfly crown ether as a phototunable supramolecular catalyst. *J. Am. Chem. Soc.* **2003**, *125* (8), 2224-2227. DOI: 10.1021/ja029331x.

(24) Dai, Z.; Cui, Y.; Chen, C.; Wu, J. Photoswitchable ring-opening polymerization of lactide catalyzed by azobenzene-based thiourea. *Chem. Commun.* **2016**, *52* (57), 8826-8829. DOI: 10.1039/C6CC04090J.

(25) Lemieux, V.; Spantulescu, M. D.; Baldridge, K. K.; Branda, N. R. Modulating the Lewis acidity of boron using a photoswitch. *Angew. Chem. Int. Ed.* **2008**, *47* (27), 5034-5037. DOI: 10.1002/anie.200800869.

(26) a) Berryman, O. B.; Sather, A. C.; Lledó, A.; Rebek, J. Switchable Catalysis with a Light-Responsive Cavitand. *Angew. Chem. Int. Ed.* **2011**, *50* (40), 9400-9403. DOI: 10.1002/anie.201105374. b) Rad, N.; Sashuk, V. A light-gated regulation of the reaction site by a cucurbit[7]uril macrocycle. *Chem. Sci.* **2022**, *13* (42), 12440-12444, 10.1039/D2SC02077G. DOI: 10.1039/D2SC02077G.

(27) a) Szewczyk, M.; Sobczak, G.; Sashuk, V. Photoswitchable Catalysis by a Small Swinging Molecule Confined on the Surface of a Colloidal Particle. *ACS Catal.* **2018**, *8* (4), 2810-2814. DOI: 10.1021/acscatal.8b00328. b) Kravets, M.; Flaibani, M.; Szewczyk, M.; Posocco, P.; Sashuk, V. Pursuing the Complete OFF State in Photoswitchable Catalysis. *ACS Catal.* **2023**, *13* (24), 15967-15976. DOI: 10.1021/acscatal.3c04435. c) Wei, Y.; Han, S.; Kim, J.; Soh, S.; Grzybowski, B. A. Photoswitchable Catalysis Mediated by Dynamic Aggregation of Nanoparticles. *J. Am. Chem. Soc.* **2010**, *132* (32), 11018-11020. DOI: 10.1021/ja104260n. d) Neri, S.; Martin, S. G.; Pezzato, C.; Prins, L. J. Photoswitchable Catalysis by a Nanozyme Mediated by a Light-Sensitive Cofactor. *J. Am. Chem. Soc.* **2017**, *139* (5), 1794-1797. DOI: 10.1021/jacs.6b12932.

(28) Martinez-Cuezva, A.; Saura-Sanmartin, A.; Nicolas-Garcia, T.; Navarro, C.; Orenes, R. A.; Alajarin, M.; Berna, J. Photoswitchable interlocked thiodiglycolamide as a cocatalyst of a chalcogeno-Baylis-Hillman reaction. *Chem. Sci.* **2017**, *8* (5), 3775-3780. DOI: 10.1039/c7sc00724h.

(29) Antoine John, A.; Lin, Q. Synthesis of Azobenzenes Using N-Chlorosuccinimide and 1,8-Diazabicyclo[5.4.0]undec-7-ene (DBU). *J. Org. Chem.* **2017**, *82* (18), 9873-9876. DOI: 10.1021/acs.joc.7b01530.

(30) Kennedy, A. D. W.; DiNardi, R. G.; Fillbrook, L. L.; Donald, W. A.; Beves, J. E. Visible-Light Switching of Metallosupramolecular Assemblies. *Chem.– Eur. J.* **2022**, *28* (16), e202104461. DOI: 10.1002/chem.202104461.

(31) August, D. P.; Nichol, G. S.; Lusby, P. J.; . Maximizing Coordination Capsule–Guest Polar Interactions in Apolar Solvents Reveals Significant Binding. *Angew. Chem. Int. Ed.* **2016**, *55*, 15022-15026. DOI: 10.1002/ANIE.201608229.

(32) Tateishi, T.; Takahashi, S.; Okazawa, A.; Martí-Centelles, V.; Wang, J.; Kojima, T.; Lusby, P. J.; Sato, H.; Hiraoka, S. Navigated Self-Assembly of a Pd_2L_4 Cage by Modulation of an Energy Landscape under Kinetic Control. *J. Am. Chem. Soc.* **2019**, *141* (50), 19669-19676. DOI: 10.1021/jacs.9b07779.

(33) Boaler, P. J.; Piskorz, T. K.; Bickerton, L. E.; Wang, J. D., F.; Lloyd-Jones, G. C.; Lusby, P. J. The Origins of High-Activity Cage-Catalyzed Michael Addition. *J. Am. Chem. Soc.* **2024**, *in press*. DOI: 10.1021/jacs.4c05160.

(34) Suzuki, K.; Kawano, M.; Fujita, M. Solvato-Controlled Assembly of Pd_3L_6 and Pd_4L_8 Coordination "Boxes". *Angew. Chem. Int. Ed.* **2007**, *46* (16), 2819-2822. DOI: 10.1002/anie.200605084.

(35) a) Preston, D.; Barnsley, J. E.; Gordon, K. C.; Crowley, J. D. Controlled Formation of Heteroleptic $Pd_2(L^a)_2(L^b)_2^{4+}$ Cages. *J. Am. Chem. Soc.* **2016**, *138* (33), 10578-10585. DOI: 10.1021/jacs.6b05629. b) Lewis, J. E. M. Multi-functional, Low Symmetry Pd_2L_4 Nanocage Libraries. *Chem.- Eur. J.* **2021**, *27* (13), 4454-4460. DOI: 10.1002/chem.202005363. c) Tarzia, A.; Lewis, J. E. M.; Jelfs, K. E. High-Throughput Computational Evaluation of Low Symmetry Pd_2L_4 Cages to Aid in System Design. *Angew. Chem. Int. Ed.* **2021**, *60* (38), 20879-20887. DOI: 10.1002/anie.202106721. d) Molinska, P.; Tarzia, A.; Male, L.; Jelfs, K. E.; Lewis, J. E. M. Diastereoselective Self-Assembly of Low-Symmetry Pd_nL_{2n} Nanocages through Coordination-Sphere Engineering. *Angew. Chem. Int. Ed.* **2023**, *62* (51), e202315451. DOI: 10.1002/anie.202315451. e) Wu, K.; Benchimol, E.; Baksi, A.; Clever, G. H. Non-statistical assembly of multicomponent Pd_2ABCD cages. *Nat. Chem.* **2024**. DOI: 10.1038/s41557-023-01415-7.

(36) The sample containing free Py* (arising from the displacement from $[Pd(Py^*)_4](BAr_F)_2$). We explored the role of Py* in the rearrangement process and found it plays no significant role when there is a significant proportion of acetonitrile in the sample (see SI S16). In nitromethane (or nitromethane/DCM mixtures) the rate of ligand exchange was still slow.